Parallel Particle-in-Cell Based Numerical Model for the Study of Terahertz Emission from Laser-Ionized Gas Targets

T. V. Liseykina

ICM&MG SBRAS
Novosibrsk

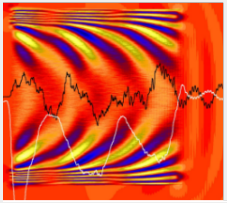

ИВМиМГ

GRID'2025
JINR, Dubna
July 7-11 2025

RSF N 24-21-00037

Radiation in the THz domain: applications

λ $10^{-3} - 10^{-1}$ см

ν $0.1 \times 10^{12} - 10 \times 10^{12}$ Гц

$\hbar\omega$ $\sim 10^{-1} - 10^{-3}$ эВ

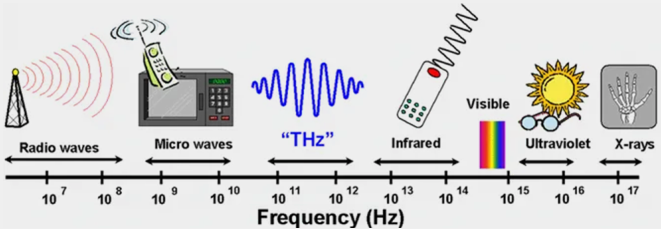

- distant probing of materials – security systems
- communication
- quality control
- noninvasive diagnostics – medicine
- plasma diagnostic
- THz spectroscopy

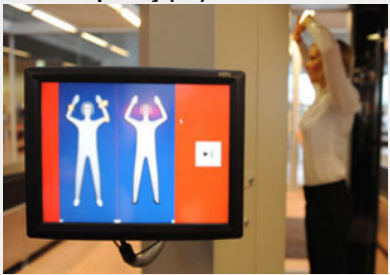

Sources of high-intensity short THz pulses

λ $10^{-3} - 10^{-1}$ cm
ν $0.1 \times 10^{12} - 10 \times 10^{12}$Hz
$\hbar\omega$ $\sim 10^{-1} - 10^{-3}$ eV

- synchrotrons
- free electron lasers
- optical rectification in crystals
- frequency conversion in plasma
- ionization-induced low-frequency currents in gases

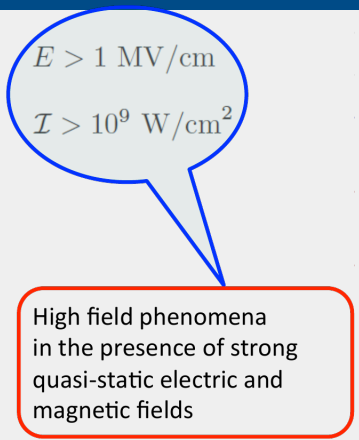

[M. Q. Bao & A.F. Starace, Static electric field effects on HHG, Phys. Rev A, 53, R3723, 1996]

How does the two-color scheme work?

Monocromatic field (long pulse)

$$\mathbf{E}(t) = \mathrm{E}_0 \cdot f(t) \cdot \cos(\omega t)$$

$$\mathbf{E}(t + T/2) = -\mathbf{E}(t)$$

$$\mathbf{j}_a(t) = -\int \mathbf{p} \cdot w_a(\mathbf{p}, t) \cdot \mathrm{d}^3 p$$

$$\mathbf{j}(t) = \sum_a \mathbf{j}_a(t)$$

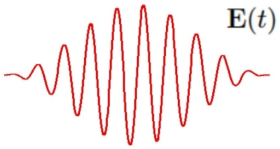

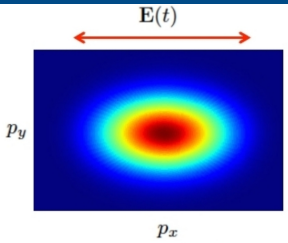

$$w(-\mathbf{p}) = w(\mathbf{p})$$

$$\langle \mathbf{j}(t) \rangle = 0$$

Non-monochromatic field

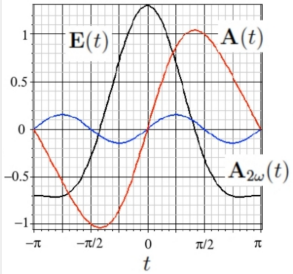

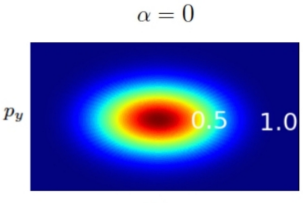

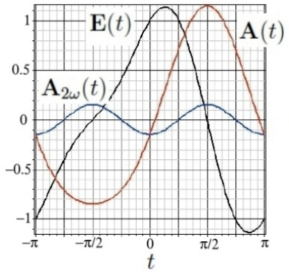

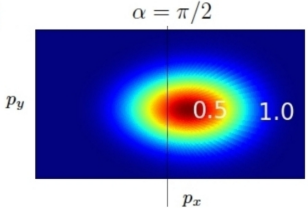

[SFA - modeling (V. Tulsky, S. Popruzhenko, D. Bauer)]

Emission from gas a target

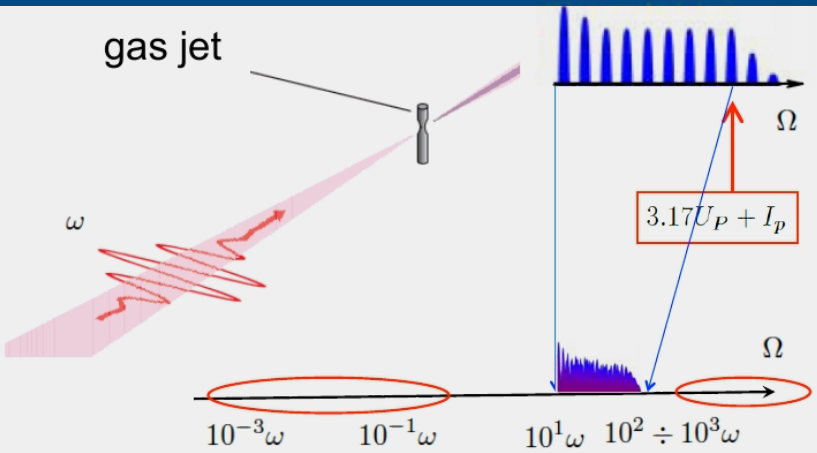

Emission from gas a target

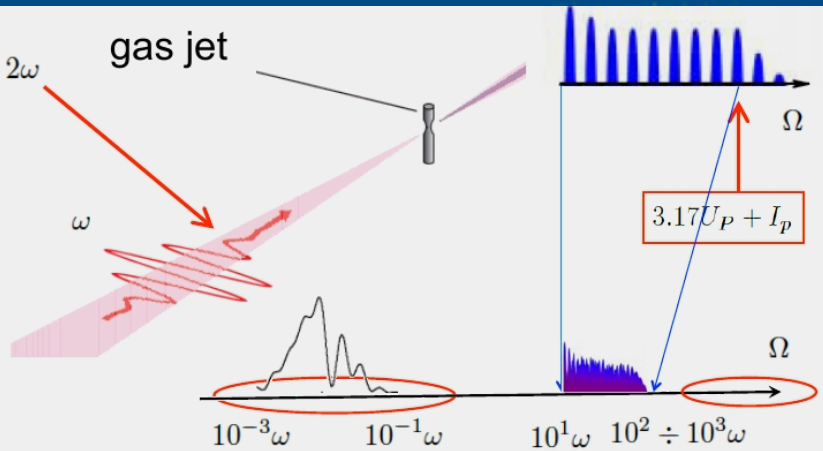

Experimental confirmations:

LANL – K. Y. Kim et al. Nat. Phot. (2008)
Maryland – T.I. Oh et al, APL (2014)
IFSA – C. Meng et al., APL (2016)
N.Novgorod – N. V. Vvedenskii et al. PRL (2014)
IESL – A. D. Koulouklidis et al., Nature Comm. (2020)

Modeling of the collective interaction

- Vlasov equations for the particles distribution functions
$$\frac{\partial f_{\mathrm{i,e}}}{\partial t} + \vec{v}\frac{\partial f_{\mathrm{i,e}}}{\partial \vec{r}} + \vec{F}_{\mathrm{i,e}}\frac{\partial f_{\mathrm{i,e}}}{\partial \vec{p}} = 0,\ \vec{F}_{\mathrm{i,e}} = q_{\mathrm{i,e}}\left(\vec{E} + \frac{1}{c}\vec{v}\times\vec{B}\right)$$
- Maxwell equations for the electromagnetic field
$$\nabla\times\vec{B} = \frac{4\pi}{c}\vec{j} + \frac{1}{c}\frac{\partial\vec{E}}{\partial t}, \quad \nabla\times\vec{E} = -\frac{1}{c}\frac{\partial\vec{B}}{\partial t},$$
$$\nabla\cdot\vec{E} = 4\pi\rho, \quad \nabla\cdot\vec{B} = 0$$
- $\vec{j} = \sum_{i,e} q_{i,e}\int f_{i,e}\vec{v}\,d\vec{v},\ \rho = \sum_{i,e} q_{i,e}\int f_{i,e}\,d\vec{v}$
- Particle-in-Cell method for the Vlasov equation
- Tunnel ionization by the electric field
$w(\mathcal{E}) = \left(\frac{2\mathcal{E}_{ch}}{\mathcal{E}}\right)^{2n^*}\frac{k^2\hbar}{m_e}\frac{\mathcal{E}}{\mathcal{E}_{ch}}\exp\left(-\frac{2\mathcal{E}_{ch}}{3\mathcal{E}}\right)$
- Immobile electron is "born"if ionization occurs
- Energy spent for ionization is accounted for by $\vec{j}_{ion}||\vec{E}_{loc}$
- Energy conservation is controlled

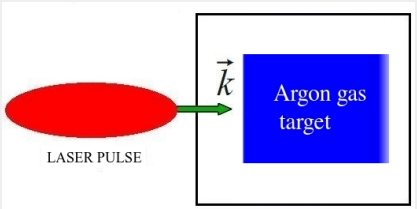

$I_\omega = 10^{14} \div 10^{15}$ W/cm^2

$\tau_{\mathrm{pulse}} \sim 250$ fs
focalspot ~ 30 μm
$\lambda_0 = 800 \div 4000$ nm
$E_{2\omega} = 0.2E_\omega$

$n_{\mathrm{Ar}} = 10^{17} \div 10^{19}$ cm^{-3}

Fields: staggered grids (Yee, Langdon& Lasinski)

- Computational domain $[x_{\min}, x_{\max}] \times [-\frac{y_{\max}}{2}, \frac{y_{\max}}{2}] \times [-\frac{z_{\max}}{2}, \frac{z_{\max}}{2}]$
- Regular Cartesian grid with spatial steps h_x, h_y, h_z
- Explicit finite-difference scheme on staggered grids
  [A. B. Langdon, B.F. Lasinski. Meth. Comput. Phys. (1976)
  K. Yee. IEEE Trans. Antennas Propag (1966)]
  field component are calculated on staggered in time and space grids
  central differences for the derivatives $\Longrightarrow \mathcal{O}(h_x^2, h_y^2, h_z^2, \tau^2)$

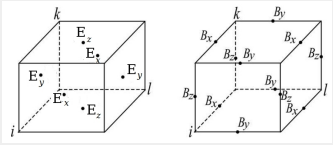

$$\begin{cases} \dfrac{\mathbf{B}^{n+\frac{1}{2}} - \mathbf{B}^{n+\frac{1}{2}}}{\tau} = -\nabla_h \times \mathbf{E}^n \\ \dfrac{\mathbf{E}^{n+1} - \mathbf{E}^n}{\tau} = \mathbf{j}^{n+\frac{1}{2}} + \nabla_h \times \mathbf{B}^{n+\frac{1}{2}} \end{cases}$$

$$\nabla_h \times \mathbf{B} = \begin{pmatrix} \dfrac{B_{z\,i,l,k-\frac{1}{2}} - B_{z\,i,l-1,k-\frac{1}{2}}}{h_y} - \dfrac{B_{y\,i,l-\frac{1}{2},k} - B_{y\,i,l-\frac{1}{2},k-1}}{h_z} \\ \dfrac{B_{x\,i-\frac{1}{2},l,k} - B_{x\,i-\frac{1}{2},l,k-1}}{h_z} - \dfrac{B_{z\,i,l,k-\frac{1}{2}} - B_{z\,i-1,l,k-\frac{1}{2}}}{h_x} \\ \dfrac{B_{y\,i,l-\frac{1}{2},k} - B_{y\,i-1,l-\frac{1}{2},k}}{h_x} - \dfrac{B_{x\,i-\frac{1}{2},l,k} - B_{x\,i-\frac{1}{2},l-1,k}}{h_y} \end{pmatrix}.$$

Particle distribution functions: Particle-in-Cell method

- plasma species are represented by a set of a large number of (macro)particles whose trajectories are characteristics of the Vlasov equations
  [Hockney, R.W & Eastwood, J.W, Computer simulation using particles. CRC Press. (2021)]

$$\frac{\mathrm{d}\vec{p}_j}{\mathrm{d}t} = \vec{F}_j, \qquad \frac{\mathrm{d}\vec{r}_j}{\mathrm{d}t} = \vec{v}_j, \qquad \vec{p}_j = \gamma m_j \vec{v}_j, \qquad \gamma = (1 - v_j^2/c^2)^{-1/2}.$$

- Lorentz force: linear interpolation between the field values in the eight (3D) or 4(2D) grid nodes nearest to the particle position $\vec{r}_j$
- Boris pusher for the equations of motion
  [J.P. Boris in: 4^{th} Conference on Numerical Simulation of Plasmas. Washington (1970)]

$$1.\quad \frac{\vec{p}_1 - \vec{p}^n}{\tau/2} = q_j \vec{E} \qquad 2.\quad \frac{\vec{p}_2 - \vec{p}_1}{\tau} = \frac{1}{c}\frac{\vec{p}_1 + \vec{p}_2}{2} \times \vec{\Omega}'$$

$$3.\quad \frac{\vec{p}_{n+1} - \vec{p}_2}{\tau/2} = q_j \vec{E}, \quad \text{with} \quad \vec{\Omega}' = \frac{\vec{\Omega}}{\sqrt{1 + p_1^2/m_j^2 c^2}}, \quad \vec{\Omega} = \frac{q_j \vec{B}}{m_j c}.$$

Parallelization scheme

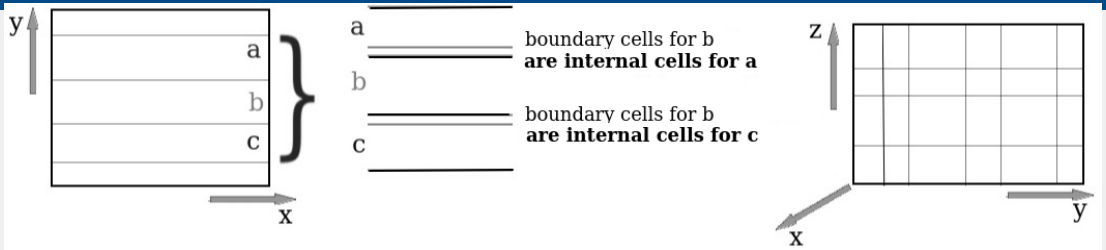

- subdomains are rectangular cuboids (3D) or rectangles stretched in the x direction (2D)
- one subdomain is assigned to one processor
- transverse sizes of the subdomains are chosen such that the load of processors is balanced
- processor stores only a part of the grid: the values of the boundary elements are passed by the processors to each other before each new time step
- at each time step, the particles that move to a cell assigned to a neighboring processor are collected and sent/received in a single block using a single MPI-SEND/MPI-RECV operation
- partial particle sorting by coordinate at each time step to achieve an efficient data exchange

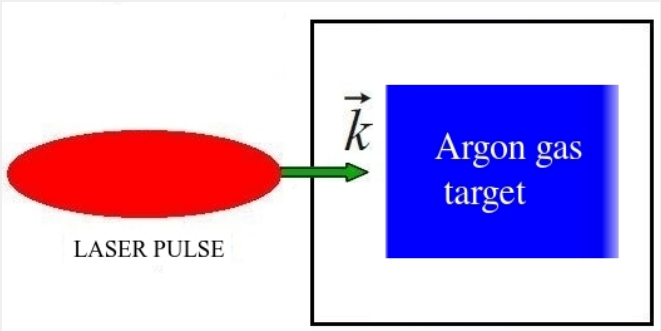
$\vec{k}$
Argon gas target
LASER PULSE

2D3V Particle-in-Cell modeling

$$\mathbf{A}(t) = \mathbf{A}_{\omega}(t) + \mathbf{A}_{2\omega}(t)$$

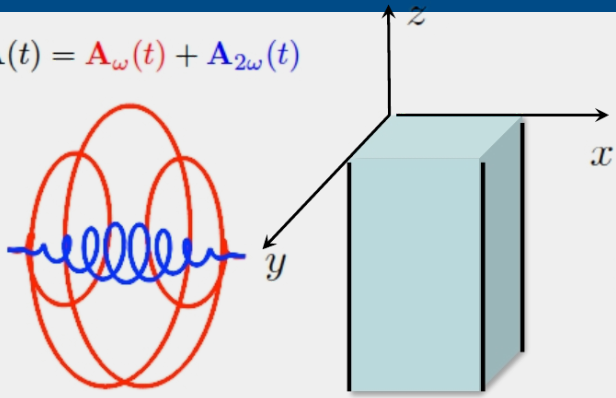

Ar

$\Delta = 20 \div 50 \mu\text{m}$

$n_e = 10^{17} \div 10^{19} \text{cm}^{-3}$

800nm

$\mathcal{I} = 2 \cdot 10^{15} \text{W/cm}^2$

$\tau_{\omega} = 250\text{fs}$

- computationally expensive
- binary collisions are not included

+ self-consistent
+ full Maxwell solver
+ tunnel ionization

Averaged electric field distribution - I

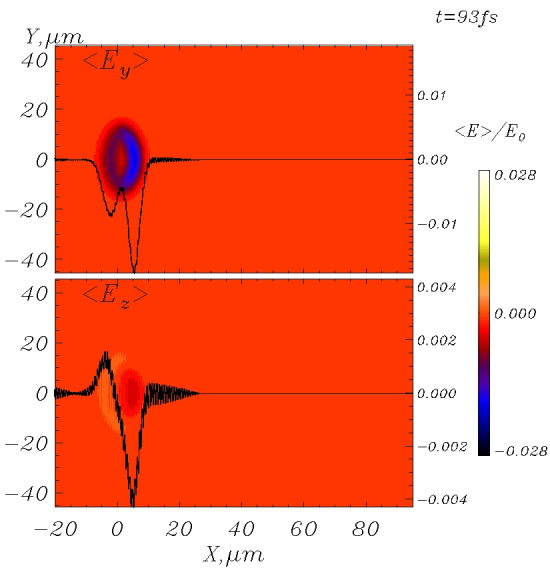

Averaged electric field distribution - I

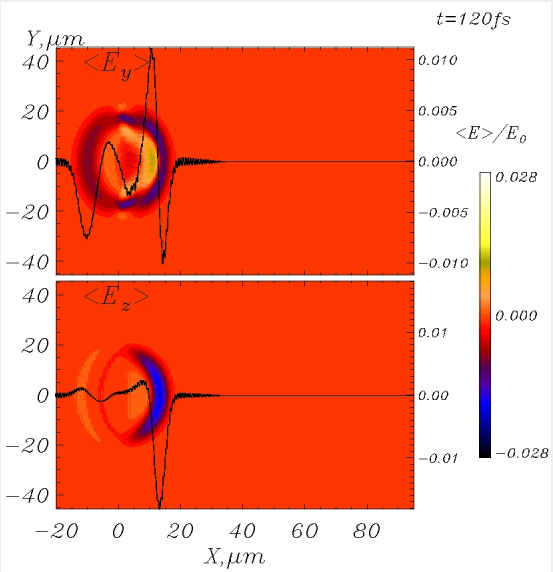

Averaged electric field distribution - I

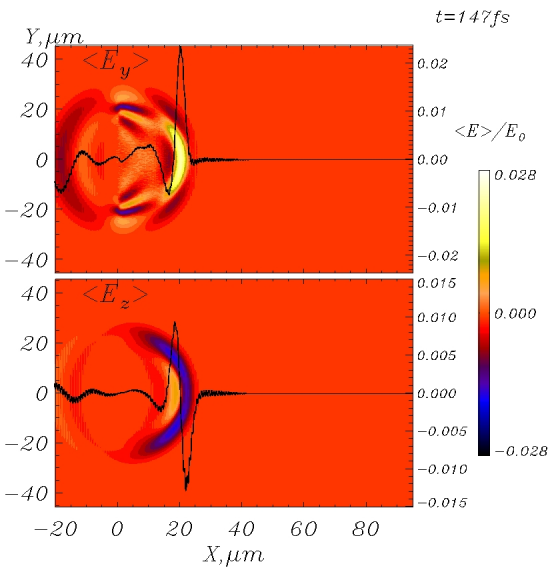

Averaged electric field distribution - I

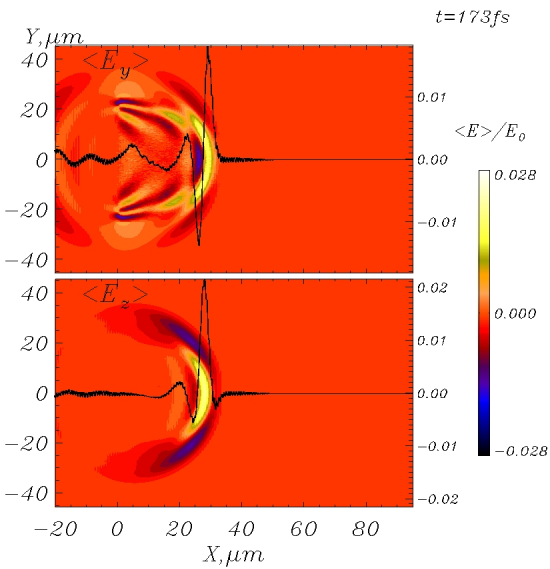

Averaged electric field distribution - I

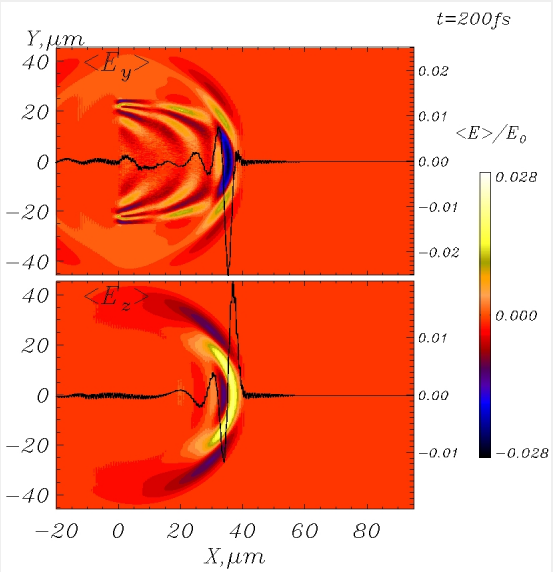

Averaged electric field distribution - I

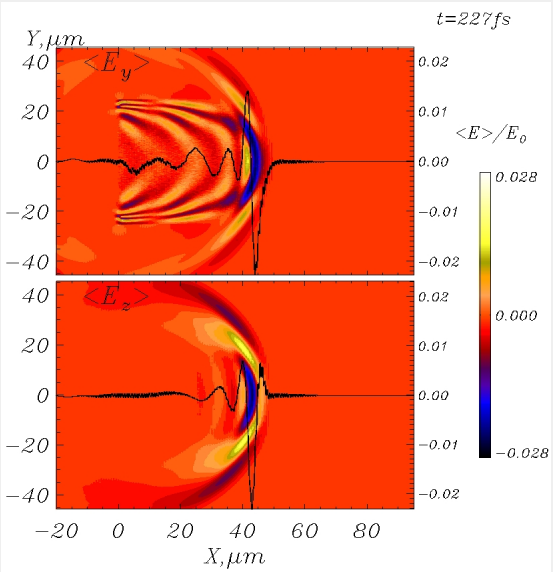

Averaged electric field distribution - I

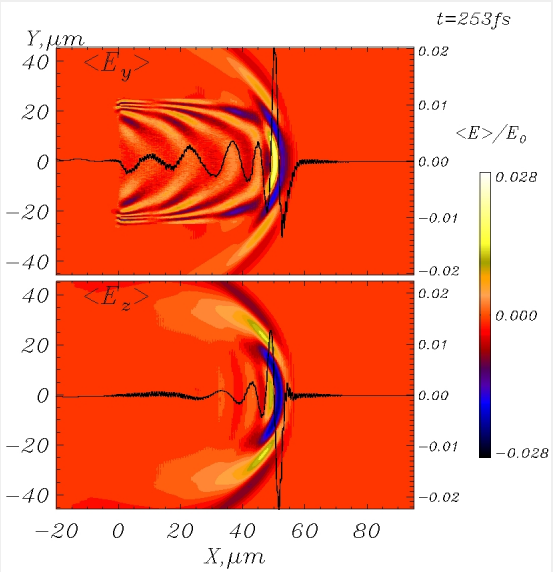

Averaged electric field distribution - I

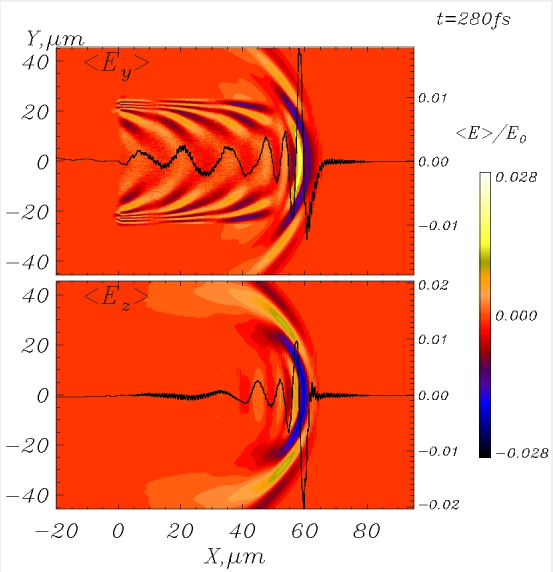

Averaged electric field distribution - I

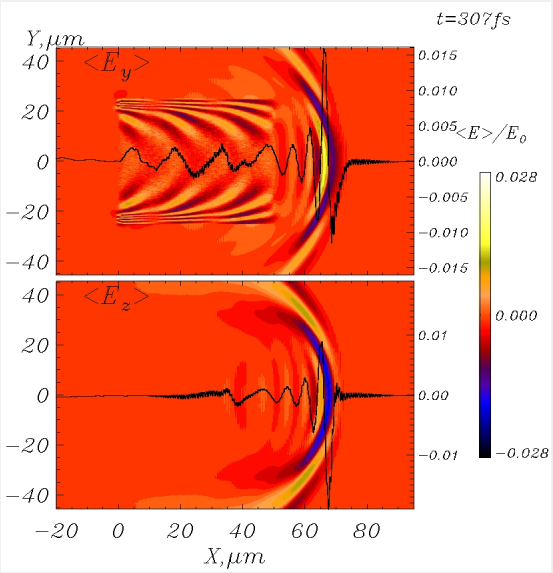

Averaged electric field distribution - I

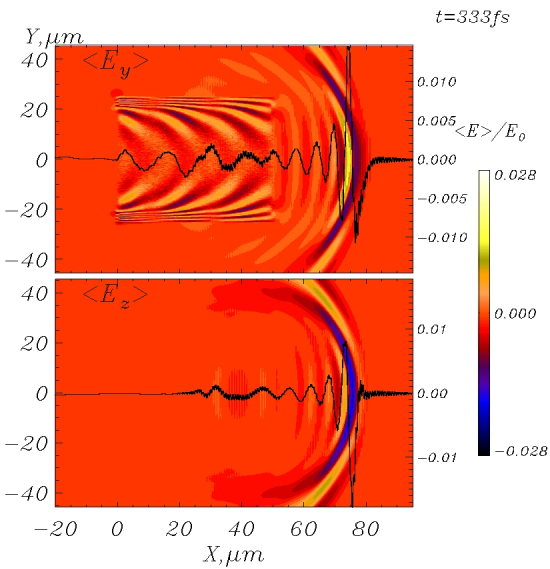

Averaged electric field distribution - I

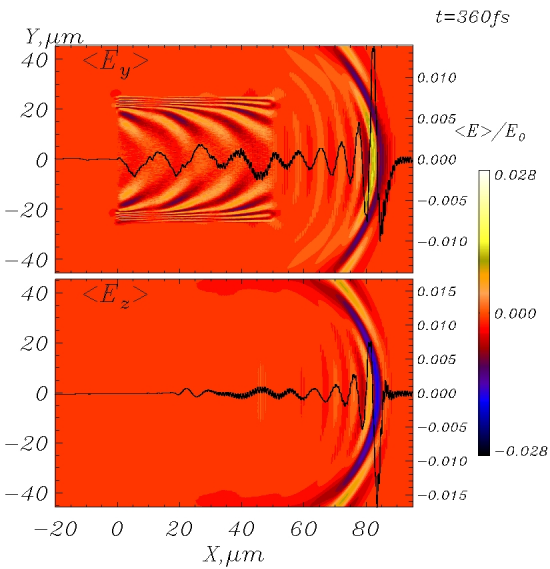

Averaged electric field distribution - II

$\Delta = 50\mu m$

$\Delta = 20\mu m$

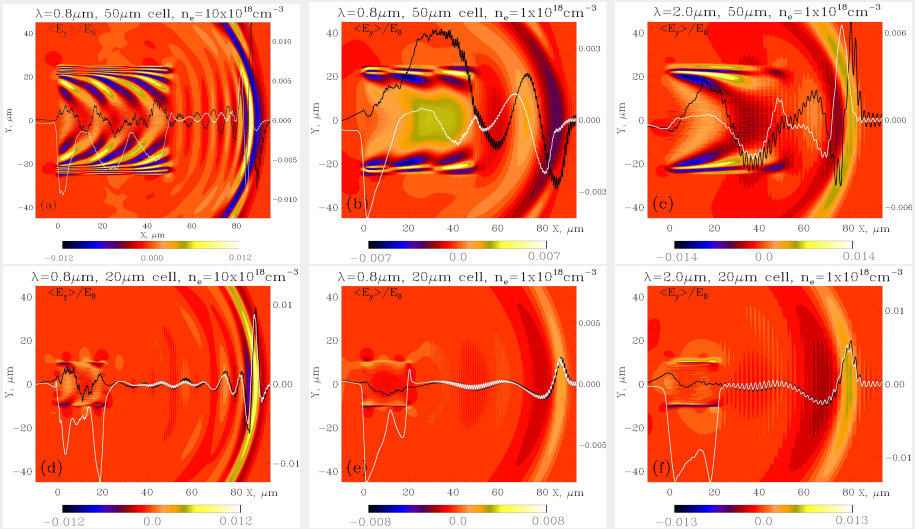

$E_{\max} = 0.01E_0 = 8.6$ MV/cm for $\lambda = 800$nm and $n_0 = 10^{19}$ cm^{-3}

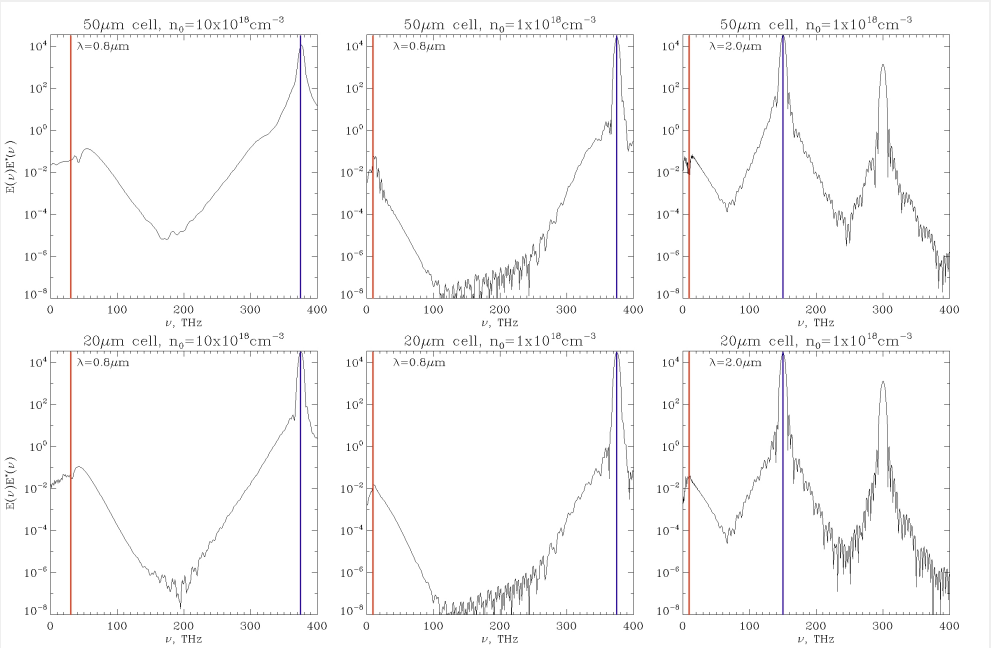
50μm cell, n0=10x10^18cm^-3
λ=0.8μm
50μm cell, n0=1x10^18cm^-3
λ=0.8μm
50μm cell, n0=1x10^18cm^-3
λ=2.0μm
20μm cell, n0=10x10^18cm^-3
λ=0.8μm
20μm cell, n0=1x10^18cm^-3
λ=0.8μm
20μm cell, n0=1x10^18cm^-3
λ=2.0μm
E(ν)E*(ν)
ν, THz

Conclusions and outlooks

- the problem of the macroscopic THz response of laser-driven plasma is address is a complimentary way by employing a particle-in-cell simulation of the plasma dynamics during and after the interaction with a non-monochromatic ionizing laser pulse
- simulation includes the ionization step and allows for a fully self-consistent calculation of the electron current including the back reaction of the coherently emitted radiation on the plasma dynamics
- high numerical costs restrict the interaction volume in all dimensions by $\sim 100\mu$m, so that the radiation emitted from a spatially restricted target is examined
  such targets can be realized with thin gas jets or small gas-filled cells [Ch. Meng et al. APL (2016)]
- the plasma dynamics is analyzed
  distributions of the quasi-static electric field inside the plasma and the radiation spectra emitted in the forward direction are calculated
  the efficiency of the electron energy conversion into that of THz radiation is estimated
- spectra in the far-field zone
- study of the dynamical non-radiation configurations

Gas-plasma-based THz generation schemes...

D. Jang et al. , "Efficient THz and brunel harmonic generation from air plasma via mid-IR coherent control". Optica, 6:1338, 2019
A. D. Koulouklidis et al., "Observation of extremely efficient THz generation from mid-IR two-color laser filaments."Nature Comm., 11:292, 2020
J. Déchard, X. Davoine, and L. Bergé "THz Generation from relativistic plasmas driven by near- to far-IR laser pulses."Phys. Rev. Lett. 123:264801, 2019
D.J. Cook & R.M. Hochstrasser. "Intense THz pulses by four-wave rectification in air."Opt. Lett., 25:1210, 2000
M. Kress et al. "THz-pulse generation by photoionization of air with laser pulses composed of both fundamental and second-harmonic waves". Opt. Lett., 29:1120, 2004
T. I. Oh et al. "Intense THz generation in two-color laser filamentation: energy scaling with terawatt laser systems". New J.Phys., 15:075002, 2013
M. Clerici et al. "Wavelength scaling of THz generation by gas ionization". Phys. Rev. Lett., 110:253901, 2013
A. Nguyen et al. "Wavelength scaling of THz pulse energies delivered by two-color air plasmas". Opt. Lett., 44:1844, 2019
V. Yu. Fedorov & S. Tzortzakis. "Optimal wavelength for two-color filamentation-induced THz sources". Opt. Express, 26:31150, 2018
A. Nguyen et al. "Broadband THz radiation from two-color mid- and far-infrared laser filaments in air. Phys. Rev. A,97:063839, 2018
A. Debayle et al. "Non-monotonic increase in laser-driven THz emissions through multiple ionization events. Phys. Rev. A, 91:041801,2015
I. Thiele et al. "Broadband THz emission from two-color femtosecond-laser-induced microplasmas."Phys.Rev. A, 96:053814, 2017
air". Optica, 2:366,

Acknowledgments

Contributors:
V.A. Vshivkov, ICM&MG SB RAS, Novosibirsk
S.V. Popruzhenko, V. Tulsky, E. Peganov, MEPhI, Moscow

Supercomputer facilities:
Joint Supercomputer Center of RAS
Siberian SuperComputer Center of the SB RAS

THANK YOU FOR YOUR ATTENTION

Conclusions ans outlooks

- несимметричная ионизация "двухцветным"лазерным полем $\Longrightarrow$ коллективные колебания в небольших мишенях
- квази-постоянное электрическое поле $E > 40$ MV/cm внутри мишени и в ближней волновой зоне
- быстрое затухание плазменных колебаний $\Longrightarrow$ короткая длительность ТГц импульса
- сохраняющиеся долгое время колебания внутри мишени
- $E_{\mathrm{m}} \sim \sqrt{n_e}\lambda$ мало зависит от размера ячейки
- сложная зависимость распределения поля от размера ячейки
- ячейка меньшено размера излучает в 2.7-4.7 раз больше энергии в пересчёте на 1 электрон
- излучение назад
- 3D моделирование для сравнения и верификации выводов из результатов 2D расчётов

Заключение – II

- Круговая поляризация предпочтительнее линейной
  Средний инфракрасный диапазон предпочтительнее инфракрасного
- Ячейки небольшого объёма эффективнее, чем протяженные
  Использование газовой струи толщиной 20 μm технически возможно!
- Существенное влияние излучения на динамику плазмы
  Формирование неизлучающих динамических конфигураций